# Time dependent Doppler shifts in high-order harmonic generation in intense laser interactions with solid density plasma and frequency chirped pulses

E. C. Welch, P. Zhang, F. Dollar, Z.-H. He, K. Krushelnick, and A. G. R. Thomas

Citation: Physics of Plasmas **22**, 053104 (2015); doi: 10.1063/1.4919857
View online: http://dx.doi.org/10.1063/1.4919857
View Table of Contents: http://scitation.aip.org/content/aip/journal/pop/22/5?ver=pdfcov
Published by the AIP Publishing



# Time dependent Doppler shifts in high-order harmonic generation in intense laser interactions with solid density plasma and frequency chirped pulses

E. C. Welch,[1,a)] P. Zhang,[1] F. Dollar,[2] Z.-H. He,[1] K. Krushelnick,[1,3] and A. G. R. Thomas[1,3,b)]
[1]*Department of Nuclear Engineering and Radiological Sciences, University of Michigan, Ann Arbor, Michigan 48109-2104, USA*
[2]*JILA, University of Colorado, Boulder, Colorado 80309, USA*
[3]*Center for Ultrafast Optical Science, University of Michigan, Ann Arbor, Michigan 48109-2104, USA*

(Received 19 February 2015; accepted 23 April 2015; published online 6 May 2015)

High order harmonic generation from solid targets is a compelling route to generating intense attosecond or even zeptosecond pulses. However, the effects of ion motion on the generation of harmonics have only recently started to be considered. Here, we study the effects of ion motion in harmonics production at ultrahigh laser intensities interacting with solid density plasma. Using particle-in-cell simulations, we find that there is an optimum density for harmonic production that depends on laser intensity, which scales linearly with $a_0$ with no ion motion but with a reduced scaling if ion motion is included. We derive a scaling for this optimum density with ion motion and also find that the background ion motion induces Doppler red-shifts in the harmonic structures of the reflected pulse. The temporal structure of the Doppler shifts is correlated to the envelope of the incident laser pulse. We demonstrate that by introducing a frequency chirp in the incident pulse we are able to eliminate these Doppler shifts almost completely. © *2015 AIP Publishing LLC*.
[http://dx.doi.org/10.1063/1.4919857]

## I. INTRODUCTION

High order harmonic generation (HHG) from laser solid-density plasma interactions has been studied extensively.[1–15] It occurs when the surface electrons of the target are oscillated by an intense laser field to relativistic speeds, where strong nonlinear effects give rise to the re-radiation at harmonics of the fundamental laser frequency.[5–9,13,15]

While much analytical work has been performed by using a simplified relativistic oscillating mirror model,[1,4] the understanding of HHG under realistic conditions is still somewhat limited. A number of previous theoretical studies in HHG considered the electron dynamics on interfaces and the scaling of the harmonics to high intensities,[1,3,4,16] however, analysis and simulations have been typically performed with static ions. However, as the laser intensity increases, it is clear that the ponderomotive push of the laser pulse will eventually cause significant ion motion during the passage of the laser pulse.[17–22] This motion will further complicate the relativistic moving mirror mechanism by adding an additional slow time scale Doppler shift to the reflected electromagnetic radiation.[10,15]

In this paper, we investigate the role of ion motion in HHG at very high laser intensities and show how the harmonic structure can be affected. We restrict our study to sharp interfaces (step function density profile) only and do not consider ionization physics, for simplicity. We show that there is an optimum density for harmonic production that depends on laser intensity, which scales linearly with the normalized vector potential $a_0 = eE_0/m_e c\omega_0$ with no ion motion but a reduced scaling if ion motion is included. We find that Doppler shifts will be present in the harmonic structures of the reflected pulse because of bulk ion motion. Furthermore, the degree of the Doppler shifts is very sensitive to the envelope of the incident laser pulse. Finally, we demonstrate a method to eliminate the Doppler shifts by including a frequency chirp in the incident pulse.

## II. RESULTS AND DISCUSSIONS

### A. Simulation configuration

We preformed a series of numerical experiments on the interaction of $\lambda_0 = 800$ nm wavelength, linearly polarized laser pulses with a steep plasma density (i.e., electron number density) profile. The laser pulses had various temporal shapes, as detailed later, all with a duration of order 10 s fs and intensity of order $10^{21}$ W cm$^{-2}$, corresponding to $a_0 \approx 30$. The reflected pulse contained rich components of high harmonics of the fundamental laser frequency, created through the relativistic oscillating mirror effect.[1–3] Our simulations were performed using a one-dimensional version of the particle-in-cell (PIC) code, EPOCH[23] (1D3P). The solid density plasma comprised of two species representing electrons and fully stripped Aluminum-27 ions. The number of particles-per-cell used was $N_{PPC} = 256$ for both species and the cell size was $\Delta x/\lambda_0 = 3 \times 10^{-3}$. The plasma density was a step function with values $n = 0$ for $0 \leq x \leq 20\lambda_0$ and $n = n_0$ for $20\lambda_0 < x < 30\lambda_0$. The effects of ion motion on the harmonic generation were investigated by comparing simulations with static (i.e., infinite mass) and mobile ions.

a)Present address: Electrical Engineering Department, University of California, Los Angeles, Los Angeles, California 90095-1594, USA.
b)agrt@umich.edu

 

### B. Determination of the optimum density for HHG

The maximum number of harmonics that can be obtained from laser solid-density plasma interactions depends on many factors such as the target plasma density, pulse length, shape, and intensity. In our previous paper,[13] we demonstrated that the scale length of an exponential plasma ramp was critical to the optimization of harmonic production. Here, we investigate an analogous scaling by keeping the density profile fixed (as a step function), but varying the plasma density to determine the optimum density for harmonic production. We use an incident Gaussian laser pulse of 20 fs full width at half maximum (FWHM) and focus only on the effects of the plasma density and pulse intensity on HHG. For a given laser intensity, higher plasma density implies a higher restoring force for plasma oscillation, which limits the amplitude of the electron surface oscillations, therefore limiting the amount of HHG by the relativistic oscillating mirror mechanism. By contrast, if the plasma density is too small, larger amplitude surface oscillations may become unstable, resulting a distortion and broadening of the HHG. Relativistically induced transparency[24,25] will occur if the density is lower than the threshold $n_e/a_0 n_c < 1$, where the plasma starts to become transmissive, so the optimum density for harmonic production must have a lower bound of $n_e > a_0 n_c$. Here, we find the optimum plasma density at which the HHG signal may be maximized but remain as a clean "picket fence" shape of high order harmonics by performing a large series of 1D simulations.

The optimum plasma density was determined by observing the largest number of clear harmonics presented in a numerical form of the Wigner transforms of the reflected pulse[26]

$$W(k,n) = \sum_{m=1}^{N} f(n+m) f^{\star}(n-m) e^{-ikm/2K}. \qquad (1)$$

Figure 1(a) shows an example of the reflected Gaussian pulse with intensity of $10^{21}$ W cm$^{-2}$ reflected from a plasma with density of $50n_c$, where $n_c$ is the non-relativistic critical density of the plasma. Its numerical Wigner transform is shown in Fig. 1(b), with harmonics up to order $15\omega_0$ displayed. *Note that only odd harmonics should be present in the Fourier spectrum but even harmonics appear in the Wigner transform.* This is because a Wigner transform is not a linear transform but causes cross terms to appear between harmonics, as in an autocorrelation.

The optimum densities for maximum number of harmonic generation are shown in Fig. 2, for particle-in-cell simulations with both static ions and mobile Al-27 ions. It was found that the optimum electron number density, $n_0$, for HHG increases as the square root of laser intensity, $I$, i.e., optimum scales approximately as $a_0$ with no ion motion but if ion motion is included then the optimum density is lower.

The $n_0 \propto a_0$ scaling can be understood in the following way. For ultrarelativistic laser-plasma regime with no ion motion, the ultrarelativistic similarity theory[4,27] states that the plasma-electron dynamics depends only on the similarity parameter $S = n_0/a_0 n_c = \text{const}$, where $n_0$ is the plasma density, which implies that the optimum plasma density for HHG should scale as $a_0$, consistent with the observed scaling. For our parameters (pulse length and density profile), a

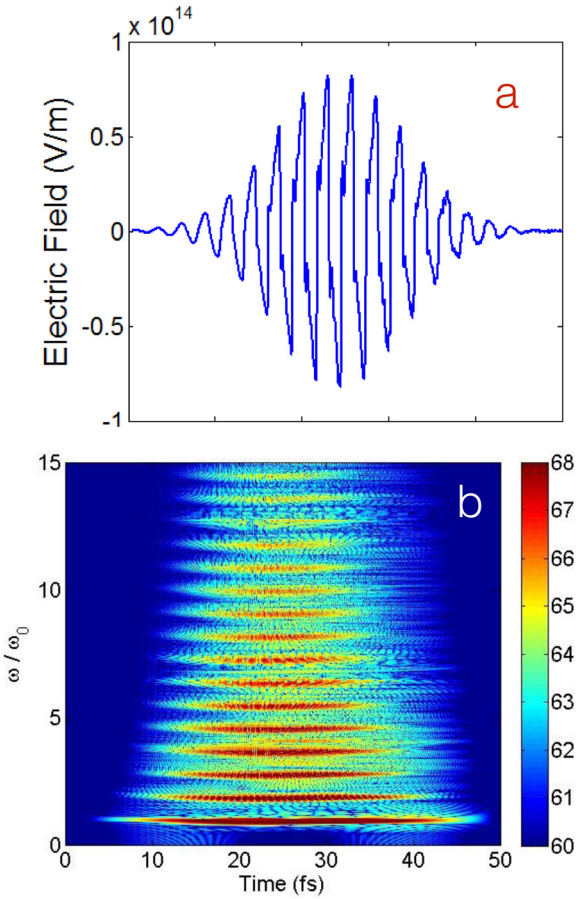


FIG. 1. Gaussian pulse with intensity of $10^{21}$ W cm$^{-2}$ reflected off plasma with density $50n_c$. The reflected pulse (top) is shown along with its Wigner transform (bottom). *As noted in the text, the Wigner transform itself generates the even harmonics observed in the figure.*

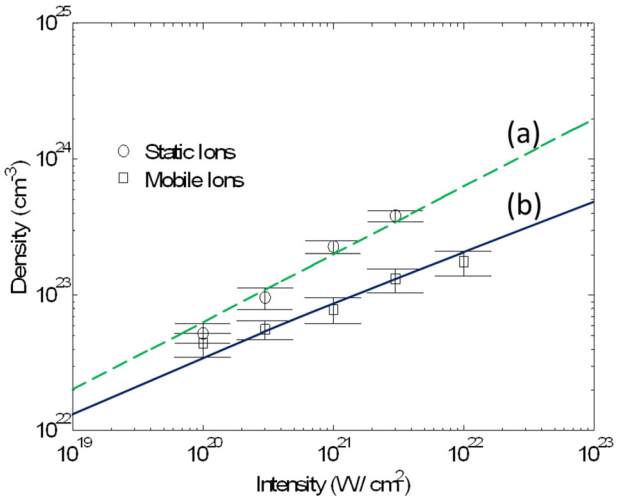


FIG. 2. Optimum densities for HHG as a function of pulse intensity from the 1D PIC simulations, for both static ions (circles) and mobile Al-27 ions (squares). Symbols represent the simulation data, error bars represent range of densities with equal number of observable harmonics, and solid lines represent the scalings described in the text fitted to the simulation data points. (a) Infinite mass ions and (b) Al-27 ions.

value of $S_0 \approx 5$ represents the optimum density as a function of intensity (extracted from the gradient of the curve labeled Fig. 2(a)).

When ion motion is included in the simulations, the optimum *initial* density is lower than in the static (infinite mass) ions case. This is because the ions are accelerated by the radiation pressure and result in a higher density at the surface where the electron surface oscillations occur. We understand this in terms of the decoupling of the two timescales: fast oscillations of electrons at the laser frequency and a slow evolution of the ion density. The standard picture of the ion motion in a semi-infinite target is that of "hole-boring"[21,22] at velocity $v_b$, i.e., the approximately constant speed at which radiation pressure drives the ion front forward in a thick target. In the rest frame corresponding to this velocity, there is a force balance between radiation pressure and the change in momentum of an incoming stream of ions with velocity $-v_b$ being reflected within a narrow region near the interface that is depleted of electrons. Making use of this frame of reference, the hole boring velocity can be shown to be[21,22]

$$\beta_b = \frac{v_b}{c} = \frac{\epsilon a_0}{1+\epsilon a_0}, \tag{2}$$

where

$$\epsilon = \sqrt{\frac{Zm_e}{m_i}\frac{n_c}{n_e}} \simeq 1.7\times 10^{-2}\sqrt{\frac{n_c}{n_e}}. \tag{3}$$

After a long time, it can be shown that the average density in the laboratory frame is $2n_0$, due to the overlap of the two ion streams with equal density $n_0' = n_0/\gamma_b$ in the hole-boring rest frame, where $\gamma_b = 1/\sqrt{1-\beta_b^2}$. Therefore, it would be expected that for a long pulse the optimum initial plasma density will be a factor of 2 lower than with infinite mass ions because of the effect of doubling of the density due to the accelerated ions. The reason for the scaling indicated by line Fig. 2(b) is because of the short pulse duration compared with the time it takes to accelerate the ions across the electron depletion region in the hole boring frame, $\tau_{acc}$.

In the hole boring frame, ions enter the electron depletion region and are reflected, leading to an increased average density in the electron depletion region (which represents the effective "spring constant" for the relativistically oscillating mirror). The flux of ions into this region over the pulse duration is $\Delta n = n_0 v_b \tau_L$. The width of the depleted region is approximately equal to $v_b\tau_{acc}$, hence, the average density of ions at the end of the pulse is

$$n = n_0 + n_0\frac{v_b\tau_L}{v_b\tau_{acc}} = n_0\left(1+\frac{\tau_L}{\tau_{acc}}\right). \tag{4}$$

By considering the longitudinal electron force balance, charge conservation and Gauss's law, Robinson *et al.*[21] give the ion acceleration time as (after substituting for the expression for $\beta_b$ above)

$$\tau_R = \frac{2m_i c}{qE_0}\sqrt{\frac{1+2\epsilon a_0}{(1+\epsilon a_0)^2}}\epsilon a_0, \tag{5}$$

where $E_0 = a_0 m_e \omega_0 c/e$ is the laser electric field. This expression was derived for circular polarization. For linear polarization (as is necessary for harmonic generation), the field will be rapidly varying between its maximum value and zero as the electron sheet moves backwards and forwards. Hence, we consider a two times longer acceleration time of $\tau_{acc} = 2\tau_R$. For $\epsilon a_0 \ll 1$ (for densities greatly exceeding $10n_c$, this condition corresponds to $a_0 \ll 1000$, which is well within the limits explored here), the factor $\sqrt{1+2\epsilon a_0/(1+\epsilon a_0)^2}$ is close to 1. Hence, we will drop this relativistic correction to the ion motion to obtain an acceleration time of

$$\tau_{acc} = \frac{4}{\omega_0}\sqrt{\frac{m_i}{Zm_e}\frac{n_c}{n_0}}. \tag{6}$$

The ultrarelativistic similarity theory does not take into account the ion motion. However, if we assume the separation of timescales between electron and ion dynamics is sufficiently distinct, the electrons will have similar dynamics for an interaction of a laser of Lorentz invariant strength $a_0$ with the surface density for $n/n_c a = S_n$, with $n$ a slowly evolving function of time. Using Eq. (4) and assuming the optimum $S_n = n/n_c a_0$ is the same as for fixed ions $S_n = S_0$, we can express the optimum density as a function of vector potential implicitly as

$$a_0 = \frac{1}{S_0}\left[\frac{n_0}{n_c} + \frac{1}{4}\sqrt{\frac{Zm_e}{m_i}}\omega_0\tau_L\left(\frac{n_0}{n_c}\right)^{3/2}\right]. \tag{7}$$

This scaling is indicated by the curve labeled (b) in Fig. 2 and shows reasonable agreement with the simulation results with ion motion. When the ion mass is taken to be infinite, this scaling reduces to the similarity theory curve (a), as it should do.

### C. Doppler shifts due to surface motion

As seen from Fig. 1(b), there is a Doppler frequency shift in the harmonics within the duration of the reflected pulse when mobile ions are used in the simulation, as would be expected of pulse reflection from a moving mirror. This net surface motion is caused by the non-negligible motion of the background ions during the laser plasma interaction. In Fig. 3, we plot the surface velocity of the electron mirror when it is impinged by laser pulses with various temporal envelopes. It is clear that the surface velocity follows closely the shape of the temporal envelope of the incident laser pulse. Also shown in Fig. 3 are the fundamental frequencies of the reflected pulse, which are obtained by looking at the peak values of the Wigner transform (the frequency of the largest magnitude for each moment in time). The frequency shifts also follow closely the envelope of the incident laser pulses. This may be easily understood as follows. When the laser intensity increases, the surface velocity also increases, which, in turn, introduces a larger frequency shift (i.e., larger Doppler red shift). Similarly, when the laser intensity decreases, the surface velocity will decrease, resulting in a smaller frequency shift.

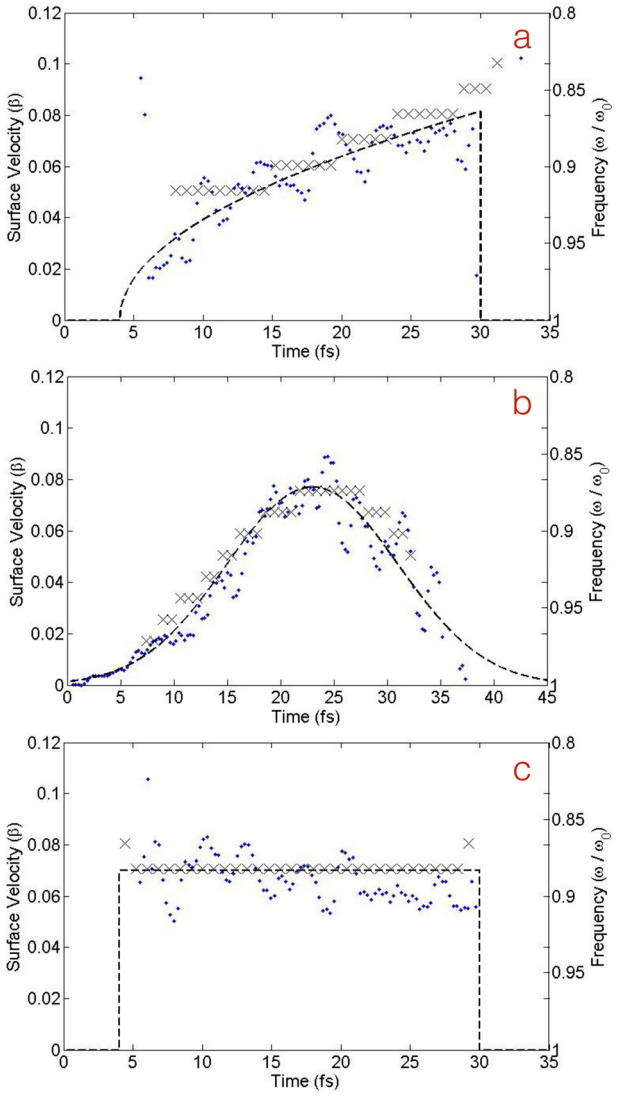


FIG. 3. Surface velocity $\beta_b = v_b/c$ (dots) and fundamental frequency of the reflected pulse (crosses) as a function of time for laser pulse with different intensity envelopes incident on targets: (a) Ramp, (b) Gaussian, and (c) Square, with target densities of $n_e = 80n_c$, $n_e = 80n_c$, and $n_e = 140n_c$, respectively, where $n_c$ is the critical plasma density at 800 nm. The dashed lines represent $a_0$ for the pulses, all of which have peak intensity of $10^{22}$ W cm$^{-2}$.

The high harmonic generation via laser-solid interaction in the presence of moving ions may be analyzed using a simple oscillating mirror model. Previous studies[2,3] assumes that the electrons at the plasma vacuum interface undergo forced oscillations around the edge of an immobile step-like ion background driven by the ponderomotive force of the incident laser pulse. Its origin is the $\vec{v} \times \vec{B}$ term of the Lorentz force, and its oscillatory term varies as $F_p(t) \propto I_L \lambda_L^2 \sin(2\omega_0 t)$. Charge separation gives rise to an electrostatic field, which serves as the restoring force. Thus, to first order, the mirror motion can be expressed as

$$X_m(\omega_0 t') = A_m \sin(2\omega_0 t' + \phi_m). \tag{8}$$

The harmonic components contained in the reflected pulses are due to the retardation effect between the point of reference (the observer) and the electron interface on which the incident wave is reflected. Assuming that the (normalized) laser field crossing the observer position is $E_{in}(t) = \sin(\omega_0 t)$, because of the retardation effect, when it returns to the observer position (after reflecting from the moving mirror surface), the wave form will become

$$E_{re}(t) = \sin(\omega_0 t - 2k_0 X_m(t')), \tag{9}$$

where $t' = t + X_m(\omega_0 t')/c$ is the retarded time, $c$ is the speed of light and $k_0$ is the laser wave number in free space.

Now consider a laser pulse with varying strength, for a plasma target with *mobile* ions. As seen from the simulation data (Fig. 3(a)), there is a surface velocity for the electron mirror that is correlated to the hole boring velocity. In the case of a ramping pulse, this surface velocity increases linearly with time, indicating an accelerating motion of the mirror surface away from the observer. By including this accelerating motion, we have

$$X_{m,v_b}(t') = A_m \sin\left[2\omega_b\left(t' - \int \beta_b dt'\right) + \phi_m\right] + \int v_b dt', \tag{10}$$

where $\omega_b = \omega_0(1 - \beta_b)$ is the laser frequency measured on the surface moving at non-relativistic speed $\beta_b$. We can Taylor expand the velocity about some reference hole boring velocity $v_{b0}$ such that

$$\int v_b dt' = v_{b0} t' + \frac{1}{2}\dot{v}_{b0} t'^2 + \cdots. \tag{11}$$

The resultant reflected wave form at the observer position can be written as

$$E_{re}(t) = \sin\left[\omega_0' t - \frac{\omega_0' \dot{v}_{b0} t^2}{c} + \cdots - 2k_0 X_m\left(\omega_0' t' - \frac{\omega_0' \dot{v}_{b0} t^2}{2c} + \cdots\right)\right], \tag{12}$$

where $\omega_0' = (1 - 2\beta_b)\omega_0$ is the (non-relativistically) Doppler shifted fundamental frequency and terms of order $\beta_{b0}^2$ have been ignored. For a non-accelerating surface, this expression is the same as Eq. (8), except with Doppler shifted fundamental frequency $\omega_0'$. The form of the expression suggests the entire harmonic structure would be Doppler shifted, consistent with the results from simulation (Fig. 3(a)). For a slowly accelerating pulse, the next order term in the expansion in Eq. (12) suggests that a linear chirp would be introduced.

The expected Doppler shift can be calculated relativistically using a relativistic expression for the hole boring velocity.[21] The instantaneous Doppler shift of the reflected wave frequency $\omega_0'$ is related to the incident frequency $\omega_0$ by

$$\frac{\omega_0'}{\omega_0} = \frac{1 - \beta_b}{1 + \beta_b} = \frac{1}{1 + 2\epsilon a_0}. \tag{13}$$

For $\epsilon a_0 \ll 1$ (true for the conditions investigated in this paper), we can express the instantaneous frequency shift due to hole boring as

$$\Delta\omega = \omega_0' - \omega_0 = 2\epsilon a_0, \tag{14}$$

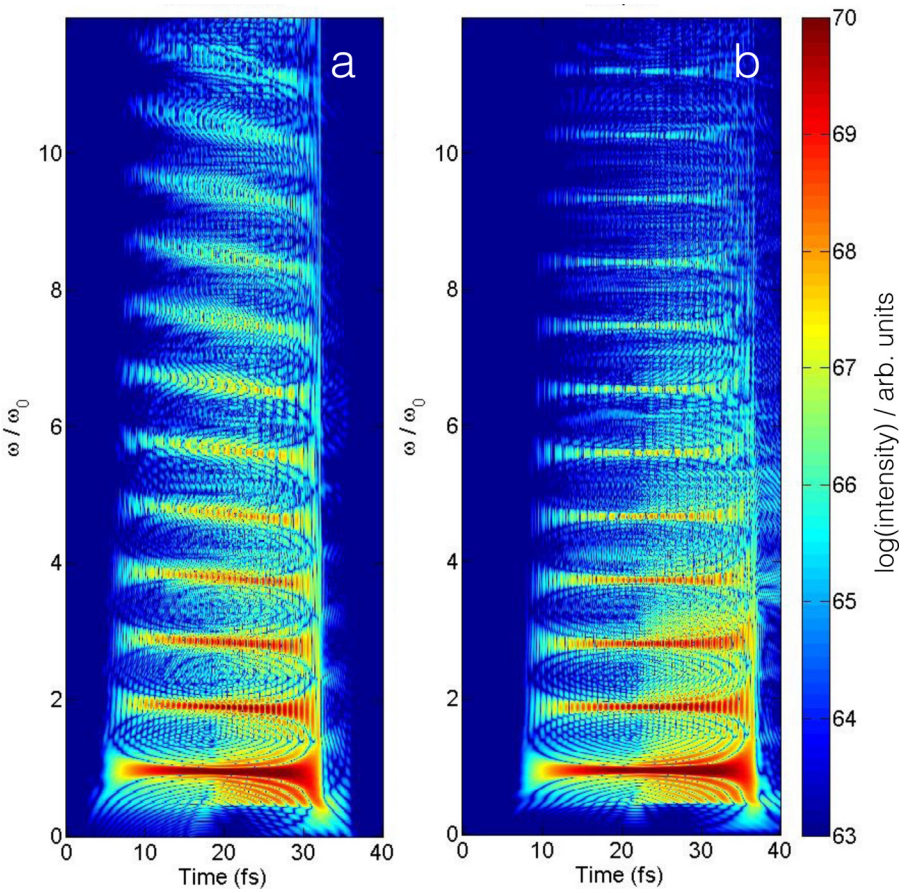


FIG. 4. Ramp pulse shape with intensity of $10^{21}$ W cm$^{-2}$ impinging on plasma with density $n_e = 44n_c$ with moving ions. Wigner transforms for reflection of (a) constant frequency pulse compared to (b) linearly chirped pulse with a 0.4% change in frequency per period, as described in the text.

which explicitly shows that the shift is proportional to the square root of laser intensity.

To characterize the effects of Doppler shifts in harmonics generation, in Fig. 4(a), we show the Wigner transform of a ramp pulse with a peak intensity of $10^{21}$ W cm$^{-2}$ and duration 20 fs after reflection from a target with density of $44n_c$. All the harmonics components are red-shifted as time increases. Note that the higher order harmonics have larger effective Doppler red shift, since the spacing between harmonics is down shifting. In the case studied here, for the 10th harmonic and above the Doppler red shift of the frequency is greater, relative to the static ions case than the laser fundamental frequency, which significantly degrades the coherence of the radiation produced. For generating coherent radiation, in particular, attosecond pulse trains, it is thus important to eliminate the Doppler red shifts observed in the harmonics.

### D. Correcting the Doppler shift of the harmonics using a chirped pulse

We found that an effective way of correcting the Doppler shifts in HHG is to introduce frequency chirps in the incident pulse. Equation (12) demonstrates that for a slowly varying laser envelope a chirp will be introduced to the reflected pulse. This can be pre-compensated by introducing an appropriate chirp to the pulse before reflection. The expected magnitude of the chirp for a ramp shaped pulse of duration $\tau_L$ can be calculated from Eq. (12) to be $(1/\omega_0')\Delta\omega/\Delta t = (v_{b0}/c)(T_L/\tau_L) \approx 0.5\%$ per laser period $T_L$. In Fig. 4(b), we show the Wigner transform for reflection of the same ramp pulse, as in Fig. 4(a), but with a linearly chirped pulse with a 0.4% change in frequency per fundamental laser period, which is in reasonable agreement with the prediction. As can be seen in the figure, the ion motion induced Doppler shifts are almost completely compensated for. For an arbitrary laser pulse intensity profile, a nonlinear chirp could be used to account for the Doppler shift.

## III. CONCLUSIONS

We have studied the effects of ion motion in harmonics production at ultrahigh laser intensities interacting with solid density plasma with a sharp interface. We found that there is an optimum initial target density for harmonic production that depends on laser intensity, which scales as $a_0$ with no ion motion but that this scaling is reduced if ion motion is included due to hole boring. We also found that Doppler redshifts will be present in the harmonic structures of the reflected pulse, because of the ion motion. The temporal dependence of the Doppler shifts follows closely the envelope of the incident laser pulse. Finally, we demonstrated that slowly accelerating ion motion induced Doppler shifts can be effectively removed by introducing a linear frequency chirp in the incident pulse.

## ACKNOWLEDGMENTS

This research was supported by the AFOSR Young Investigator Program through Award No. FA9550-12-1-0310, AFOSR Grant No. FA9550-14-1-0309, the National

Science Foundation through Grant No. PHY-1054164, the Department of Energy through Grant No. DE-SC0008352, and in part through computational resources and services provided by Advanced Research Computing at the University of Michigan, Ann Arbor. The EPOCH code was developed as part of the UK EPSRC funded projects EP/G054940/1. Simulations were performed on Flux at the University of Michigan.

[1]R. Lichters, J. MeyerterVehn, and A. Pukhov, Phys. Plasmas **3**, 3425 (1996).
[2]G. D. Tsakiris, K. Eidmann, J. Meyer-ter Vehn, and F. Krausz, New J. Phys. **8**, 19 (2006).
[3]S. Gordienko, A. Pukhov, O. Shorokhov, and T. Baeva, Phys. Rev. Lett. **93**, 115002 (2004).
[4]T. Baeva, S. Gordienko, and A. Pukhov, Phys. Rev. E **74**, 065401(R) (2006).
[5]S. V. Bulanov, N. M. Naumova, and F. Pegoraro, Phys. Plasmas **1**, 745 (1994).
[6]D. von der Linde and K. Rzazewski, Appl. Phys. B: Lasers Opt. **63**, 499 (1996).
[7]P. A. Norreys, M. Zepf, S. Moustaizis, A. P. Fews, J. Zhang, P. Lee, M. Bakarezos, C. N. Danson, A. Dyson, P. Gibbon *et al.*, Phys. Rev. Lett. **76**, 1832 (1996).
[8]L. Plaja, L. Roso, K. Rzazewski, and M. Lewenstein, J. Opt. Soc. Am. B: Opt. Phys. **15**, 1904 (1998).
[9]N. Naumova, I. Sokolov, J. Nees, A. Maksimchuk, V. Yanovsky, and G. Mourou, Phys. Rev. Lett. **93**, 195003 (2004).
[10]F. Quéré, C. Thaury, J. P. Geindre, G. Bonnaud, P. Monot, and P. Martin, Phys. Rev. Lett. **100**, 095004 (2008).
[11]B. Dromey, M. Zepf, A. Gopal, K. Lancaster, M. S. Wei, K. Krushelnick, M. Tatarakis, N. Vakakis, S. Moustaizis, R. Kodama *et al.*, Nat. Phys. **2**, 456 (2006).
[12]C. Roedel, D. an der Bruegge, J. Bierbach, M. Yeung, T. Hahn, B. Dromey, S. Herzer, S. Fuchs, A. G. Pour, E. Eckner *et al.*, Phys. Rev. Lett. **109**, 125002 (2012).
[13]F. Dollar, P. Cummings, V. Chvykov, L. Willingale, M. Vargas, V. Yanovsky, C. Zulick, A. Maksimchuk, A. G. R. Thomas, and K. Krushelnick, Phys. Rev. Lett. **110**, 175002 (2013).
[14]S. Kahaly, S. Monchoce, H. Vincenti, T. Dzelzainis, B. Dromey, M. Zepf, P. Martin, and F. Quere, Phys. Rev. Lett. **110**, 175001 (2013).
[15]H. Vincenti, S. Monchoce, S. Kahaly, G. Bonnaud, P. Martin, and F. Quere, Nat. Commun. **5**, 3403 (2014).
[16]D. an der Brugge and A. Pukhov, Phys. Plasmas **14**, 093104 (2007).
[17]J. Denavit, Phys. Rev. Lett. **69**, 3052 (1992).
[18]S. C. Wilks, W. L. Kruer, M. Tabak, and A. B. Langdon, Phys. Rev. Lett. **69**, 1383 (1992).
[19]N. Naumova, T. Schlegel, V. T. Tikhonchuk, C. Labaune, I. V. Sokolov, and G. Mourou, Phys. Rev. Lett. **102**, 025002 (2009).
[20]T. Schlegel, N. Naumova, V. T. Tikhonchuk, C. Labaune, I. V. Sokolov, and G. Mourou, Phys. Plasmas **16**, 083103 (2009).
[21]A. P. L. Robinson, P. Gibbon, M. Zepf, S. Kar, R. G. Evans, and C. Bellei, Plasma Phys. Controlled Fusion **51**, 024004 (2009).
[22]A. Macchi, M. Borghesi, and M. Passoni, Rev. Mod. Phys. **85**, 751 (2013).
[23]See http://ccpforge.cse.rl.ac.uk/gf/project/epoch/ for Epoch: Extendable PIC open collaboration.
[24]F. Cattani, A. Kim, D. Anderson, and M. Lisak, Phys. Rev. E **62**, 1234 (2000).
[25]S. Palaniyappan, B. M. Hegelich, H. Wu, D. Jung, D. C. Gautier, L. Yin, B. J. Albright, R. P. Johnson, T. Shimada, S. Letzring *et al.*, Nat. Phys. **8**, 763 (2012).
[26]A. Swami, J. M. Mendel, and C. L. Nikias, *Higher-Order Spectral Analysis Toolbox User's Guide* (MathWorks, Inc., 1993).
[27]S. Gordienko and A. Pukhov, Phys. Plasmas **12**, 043109 (2005).